HHS Public Access

Author manuscript

J Bone Miner Res. Author manuscript; available in PMC 2022 November 01.

Published in final edited form as:

J Bone Miner Res. 2021 November ; 36(11): 2229–2242. doi:10.1002/jbmr.4423.

Plasminogen regulates fracture repair by promoting the functions of periosteal mesenchymal progenitors

Luqiang Wang[1,2,*], **Lutian Yao**[1,3,*], **Hao Duan**[4,5,6,*], **Fan Yang**[4], **Maohuan Lin**[4], **Rongxin Zhang**[5], **Zhenqiang He**[5], **Jaimo Ahn**[1], **Yi Fan**[5], **Ling Qin**[1,#], **Yanqing Gong**[4,#]

[1]Departments of Orthopaedic Surgery, Perelman School of Medicine, University of Pennsylvania, Philadelphia, Pennsylvania 19104, USA

[2]Department of Orthopaedics, National Cancer Center/National Clinical Research Center for Cancer/Cancer Hospital, Chinese Academy of Medical Sciences and Peking Union Medical College, Beijing 100021, China.

[3]Department of Orthopaedics, The First Hospital of China Medical University, Shenyang 110001, China.

[4]Division of Translational Medicine and Human Genetics, Perelman School of Medicine, University of Pennsylvania, Philadelphia, PA 19104, USA

[5]Department of Radiation Oncology, Perelman School of Medicine, University of Pennsylvania, Philadelphia, Pennsylvania 19104, USA

[6]Departments of Neurosurgery, Sun Yat-Sen University Cancer Center, State Key Laboratory of Oncology in South China, Collaborative Innovation Center for Cancer Medicine, Guangzhou, 510060, China

Abstract

Defective or insufficient bone repair and regeneration are common in patients as a result of major trauma or severe disease. Cell therapy with periosteal mesenchymal progenitors, which can be limited in severe injury, serves as a promising approach; however, its efficacy is limited due to a repair-hostile ischemic tissue microenvironment after traumatic fracture. Here we report that plasminogen (Plg), a factor that is upregulated in these environments, is critical for fracture healing. Plg knockout mice had impaired trabecular and cortical bone structure, and exhibited delayed and incomplete fracture healing. Interestingly, Plg deficiency greatly reduced the thickness of expanded periosteum, suggesting a role of Plg in periosteal mesenchymal progenitor-mediated bone repair. In culture, Plg increased cell proliferation and migration in periosteal mesenchymal progenitors and inhibited cell death under ischemic conditions. Mechanistically, we revealed that Plg cleaved and activated Cyr61 to regulate periosteal progenitor function. Thus, our

[#]Correspondence to: Dr. Ling Qin, and Dr. Yanqing Gong., **Ling Qin, PhD.** Department of Orthopaedic Surgery, Perelman School of Medicine, University of Pennsylvania, G14A Stemmler Hall, 36th Street and Hamilton Walk, Philadelphia, PA 19104, USA. Tel.: (215) 898-6697; Fax: (215) 573-2133; qinling@pennmedicine.upenn.edu. **Yanqing Gong, PhD.** Division of Translational Medicine and Human Genetics, Perelman School of Medicine, University of Pennsylvania, PA 19104, USA. Tel.: (215) 746-3510; Fax: 215-573-8606; gongy@pennmedicine.upenn.edu.

[*]Co-first authors: Luqiang Wang, Lutian Yao, and Hao Duan.

Disclosures: The authors have declared that no conflict of interest exists.

study uncovers a cellular mechanism underlying fracture healing, by which Plg activates Cyr61 to promote periosteal progenitor proliferation, survival and migration and improves bone repair after fracture. Targeting Plg may offer a rational and effective therapeutic opportunity for improving fracture healing.

Introduction

Bone is a unique tissue that completely regenerates, rather than healing with a scar, after injury unlike many other tissues[1]. However, insufficient bone repair and regeneration are also common in patients with major trauma or severe illness[2]. The promotion of endogenous bone repair after fracture remains a big challenge in the clinical setting. Bone regeneration is a complex process involving cells and factors from various bone compartments. Mesenchymal progenitors from periosteal, endosteal, or marrow compartments are the primary cell source for bone repair [3].During fracture healing, mesenchymal progenitors migrate to the injury site, and proliferate and differentiate to cartilage-forming chondrocytes and bone-forming osteoblasts to directly partake in bone repair[4]. However, the regulatory mechanism underlying the actions of mesenchymal progenitors during bone repair remains largely unknown. A better understanding of these mechanisms may lead to discovery of new therapeutic targets for improving bone repair.

Plasminogen/Plasmin (Plg/Plm) is a primary enzyme for blood clot dissolution. Plg is an inactive proenzyme that can be converted to the active serine protease plasmin by tissue-type plasminogen activator (tPA) and urokinase-type PA (uPA). Plasminogen activator inhibitor 1 (PAI-1), the primary endogenous inhibitor of tPA and uPA, suppresses clot lysis. Despite its traditional role for regulation of blood coagulation, Plg has been reported to play a requisite role in post-injury repair of a variety of tissue [5–8]. Recent work by our group and others has identified that Plg regulates tissue repair through mediating cell mobilization and migration in macrophages, stem cells as well as smooth muscle cells [6,9,10]. As a thrombolytic agent, tPA or ocriplasmin, a truncated form of Plm with intact enzyme activity but eliminated bleeding side-effect, has been clinically utilized for treating myocardial infarction or vitreomacular adhesion, respectively [11–14].

It has been long recognized that tPA, uPA and PAI-1 also participate in bone metabolism. Analyzing tPA and uPA knockout (KO) mice revealed the role of Plg activators in regulating osteoblast and osteoclast activities [15,16]. Recent studies showed that bone repair is delayed in tPA KO but not in uPA KO mice [17]. Meanwhile, PAI-1 deficient mice are resistant to ovarietomy (ovx)-induced osteoporosis [18] and have increased callus formation after fracture [19]. Recent studies on Plg-deficient mice also demonstrated its important roles in bone metabolism and regeneration. Plg KO mice have reduced bone mineral density due to increased bone resorption caused by suppressed OPG expression from osteoblasts [20]. Bone repair is delayed or blocked in Plg KO mice due to drastically reduced vascularization at the chondro-osseous junction in callus. This defect was attributed to deceased VEGF expression in one report [8] and the accumulation of fibrin in another one [21]. Plm is well known for its ability to regulate cell proliferation and migration by degrading multiple extracellular matrix (ECM) proteins and activating other proteases to liberate growth factors and cytokines from

ECM [9,22–25]. In order to understand the role of the plasminogen pathway in fracture healing, in this study, we applied closed, midshaft tibial fracture with a weight-drop device, a clinically relevant traumatic fracture model, in Plg deficient mice. The healing process was characterized over time in comparison with WT mice. The regulatory actions of Plg on periosteal mesenchymal progenitors, as well as the underlying molecular mechanisms, were investigated during bone repair. Our study revealed that Plg regulates bone repair after facture through modulation of cell proliferation and migration in periosteal mesenchymal progenitors.

Material and Methods

Animals and fracture surgery.

The widetype ($Plg^{+/+}$) and Plg-deficient ($Plg^{-/-}$) mice in B6 background were bred by using Plg-heterozygous mice and offspring were genotyped by PCR as previously described [26]. In accordance with the standards for animal housing, mice were group housed at 23–25°C with a 12 h light/dark cycle and allowed free access to water and standard laboratory pellets. At 2 months of age, male $Plg^{+/+}$ and $Plg^{-/-}$ mice received closed transverse fractures at right tibiae via a blunt guillotine with a pre-inserted intramedullary pin as we described previously [27]. Fractured tibiae were harvested at various time points for microCT imaging, histology analysis, and mechanical testing. Investigators were blinded during allocation, animal handling, and endpoint measurements. All animal experiments were performed in accord with protocols approved by the Institutional Animal Care and Use Committee.

Micro-computed tomography (microCT) analysis.

Femurs from normal, uninjured 2-month-old male mice were harvested and scanned by microCT 35 (Scanco Medical AG, Brüttisellen, Switzerland). For trabecular bone analysis, the distal end of the femur corresponding to a 0 to 4.1 mm region above the growth plate was scanned at 6 μm isotropic voxel size to acquire a total of 686 μCT slices per scan. All images were smoothened by a Gaussian filter (sigma=1.2, support=2.0) and then thresholded corresponding to 491.98 mg HA/cm^3. The images of the secondary spongiosa regions located at 0.6–1.8 mm below the lowest point of the growth plate were contoured for trabecular bone analysis. Bone volume fraction (BV/TV), trabecular thickness (Tb.Th), trabecular separation (Tb.Sp), trabecular number (Tb.N) and structure model index (SMI), were calculated by 3D standard microstructural analysis. For cortical bone analysis, the midshaft region (1 mm total at the midline of femur) was scanned at 6 μm isotropic voxel size. All images were smoothened by a Gaussian filter (sigma=1.2, support=2.0) and then thresholded corresponding to 668.97 mg HA/cm^3. Cortical thickness (Ct.Th), cortical tissue mineral density (TMD), polar moment of inertia (pMOI), cortical area (Ct.Ar), porosity, periosteal perimeter (Ps.Pm), and endosteal perimeter (Ec.Pm) were measured using the micro-CT scanner software (Scanco Medical).

Fractured tibiae harvested at 5, 7, 10, 14, 28, and 42 days post injury were scanned for callus analysis using VivaCT 40 (Scanco Medical AG, Brüttisellen, Switzerland) with a 10.5 μm isotropic voxel size. A total of 686 μCT slices centering on the fracture site were chosen to include the fracture callus in all dimensions. A semi-automated contouring method was

used to determine the callus perimeter and analyze the callus outside the pre-existing cortical bone. All images were first smoothed by a Gaussian filter (sigma=1.2, support=2.0) and then applied a threshold corresponding to 333.62 mg HA/cm^3 to distinguish mineralized tissue from nonmineralized and poorly mineralized tissue. Total callus volume (TV), bone volume (BV), and bone volume fraction (BV/TV) were measured using 3D standard microstructural analysis. Based on microCT images, tibiae at day 42 post injury were assigned fracture healing scores according to a modified five-point radiographic scoring system [(28)].

Mechanical testing.

Tibiae at 42 days post fracture were harvested for mechanical testing using an Instron 5542 (Instron, Norwood, MA, USA). Tibiae were positioned so that the loading point was at the fracture site. A load speed of 1.8 mm/min was applied midway between two supports placed 10 mm apart. Peak load, stiffness, and energy to failure were calculated from the force-to-failure curve.

Histology and immunohistochemistry (IHC).

Fractured tibiae were fixed in 4% paraformaldehyde for 2 days, rinsed with running water, and then decalcified in 10% EDTA (PH7.4) for 3 weeks prior to paraffin embedding. A series of 6 μm-thick longitudinal sections were cut across the entire fracture callus from one side of cortical bone to the other side of cortical bone. The section with the largest callus area and another two sections at 192 μm (about 1/4 bone width) before and after the selected section were chosen for Safranin-O/Fast green staining and quantification. Callus area, cartilage area and bone area were quantified by ImageJ. Additional sections neighboring the central section were used for IHC. After antigen retrieval, primary antibodies were added to the slices and incubated at 4°C overnight, followed by biotinylated secondary antibodies treatment and DAB color development. The first antibodies used in this study are: rat anti-Endomucin (Santa Cruz Biotechnology, Dallas, TX, USA; sc-65495), goat anti mouse fibrin (Nordic Immunology, Tibury, Northerland; GAM/Fbg). For TRAP staining, tartrate-resistant acid phosphatase (TRAP) assay kit (Sigma-Aldrich, St. Louis, MO, USA; 387A-1KT) was used.

Frozen sections were used for immunofluorescent imaging. Tibiae were harvested and fixed in 4% paraformaldehyde for 1 day, rinsed with running water, transferred to 30% sucrose in PBS overnight, and embedded in OCT compound (Thermo Fisher Scientific, Waltham, MA, USA). 6 μm-thick sections were cut with cryofilm 2C (SECTION-LAB Co. Ltd., Hiroshima, Japan). For EdU staining, EdU was injected with 1.6 mg/kg dosage at 3 hr before sacrifice and the staining was carried out according to the manufacturer's instructions (Click-iT™ EdU Alexa Fluor™ 647 Imaging Kit, Thermo Fisher Scientific, Waltham, MA, USA; c10340). Images were taken with a Nikon Eclipse 90i fluorescence microscope. *Depletion of Plg in FBS*. FBS was passed over Lysine-Sepharose 4B columns (17–0690-01, GE Healthcare) several times and the flow-through fraction was collected [(29)]. Depletion of Plg was confirmed by bovine plasminogen activity kit (EBP2211–1, AssayPro). To confirm Plg depletion in Plg$^{-/-}$ mice, plasma of Plg$^{+/+}$ or Plg$^{-/-}$ mice were collected and subjected to ELISA assay by mouse Plasminogen activity kit (EMP2211–1, AssayPro).

Periosteal mesenchymal progenitor culture.

Intact tibiae from 2-month-old male mice (>= 6 mice per experiment) were harvested for periosteal mesenchymal progenitor culture. After dissected the surrounding tissue and both ends, the tibiae were place in digestion medium containing 2 mg/mL collagenase A and 2.5 mg/mL trypsin at 37°C. The digestion medium was changed after the first 3 min of digestion. After digestion, cells were collected and cultured in the growth medium (αMEM supplemented with 15% FBS, 55 μM β-mercaptoethanol, 2 mM glutamine, 100 IU/ml penicillin and 100 μg/ml streptomycin). For colony-forming unit fibroblast (CFU-F) assay, cells were seeded in T25 flask (5×10^6 cells per flask) in normal FBS or Plasminogen-depleted FBS for 1 week, and then stained with 0.3% crystal violet in methanol. Colony numbers and diameters were quantified. For osteogenic differentiation assay, cells were seeded (3×10^6 per well) in 6-well plate. After reach 80~90% confluence, cells were switched to osteogenic medium (αMEM with 10% FBS, 10 nM dexamethasone, 10 mM β-glycerophosphate, 50 μg/mL ascorbic acid, 100 IU/ml penicillin and 100 μg/ml streptomycin) for 2 weeks followed by alizarin red staining. 3-D culture method was used for chondrogenic differentiation. Aliquots of progenitor cell solution in chondrogenic medium (high glucose DMEM, 100 μg/ml sodium pyruvate, 1% ITS+ Premix, 50 μg/ml ascorbate-2-phosphate, 40 μg/ml L-proline, 0.1 mM dexamethasone, 10 ng/ml TGF-β3, 100 IU/ml penicillin and 100 μg/ml streptomycin) were distributed to a V-bottomed 96-well plate followed by centrifugation at 300G for 5 minutes to form pellet. Pellets were cultured for 3 weeks, then embedded in paraffin for Alcian blue staining.

Cell proliferation assay.

Periosteal progenitor cells were seeded on 96-well plates at a density of 3000 cells/well under normoxia at 37 °C in a humidified air atmosphere with 5% CO_2, and allowed to attach for 16 hours. For cell proliferation, culture medium was replaced with α-MEM supplemented with 1% FBS with or without addition of Plg (HPG2070, Enzyme Research Laboratories) and PBS, or IgG or anti-Cyr61 antibody (MAB4864, R&D systems). Cells were incubated under hypoxia (5% O_2) at 37 °C in a humidified air atmosphere with 5% CO_2 for 24 or 48 hours. Cell viability was determined by MTS assay (Abcam, ab197010) according to the manufacturer's instructions.

Cell migration assay.

Periosteal progenitor cells were seeded (3×10^4 cells/well) on transwell (8 μm–pore, Falcon, 353097) in a 24-well plate in serum-free culture medium. Plg with PBS or IgG or anti-Cyr61 antibody (20 μg/ml) were added into the inserts. Cell migration was induced by adding 1% FBS in the bottom chamber under hypoxia (5% O_2). Six hours later, cells on the top of membrane were swiped off by cotton swab. Membrane of inserts then fixed in methanol and stained with Toluidine Blue (198161, Sigma-Aldrich) for 5 minutes. Images were taken in 3~4 fields per well under microscope and migrated cells on the bottom of the membrane were counted by ImageJ software.

For cell migration with siRNA Integrin β5, periosteal progenitor cells were transfected with 20 nM of either negative control siRNA (AM4611, Thermo Fisher Scientific) or siRNA

targeting Integrin beta5 (155913, Thermo Fisher Scientific), followed by cell migration assay described above.

Apoptosis Assay.

Periosteal progenitor cells were seeded on 6-well plates at a density of 2×10^5 cells/well under normoxia at 37 °C in a humidified air atmosphere with 5% CO_2, and allowed to attach for 16 hours. Culture media was replaced with serum-free growth medium with 0.03% BSA with or without Plg (10 or 20 μg/ml) and cells were incubated under hypoxia (2% O_2) at 37 °C in a humidified air atmosphere with 5% CO_2 for 48 hours. Cells were collected and stained using FITC Annexin V Apoptosis Detection Kit I (BD Pharmingen™, 556547) according to the manufacturer's specifications. FACS analysis was performed using an Accuri C6 flow cytometer (BD Biosciences).

RNA analysis of marker genes.

For RNA analysis, cells were collected in Tri Reagent (Sigma Aldrich, St. Louis, MO, USA) for RNA purification. Transcribe mRNA was reversed to cDNA using a Taqman Reverse Transcription Kit (Applied BioSystems, Inc., Foster City, CA, USA), and subsequently analyzed by SYBR green-based real-time PCRs using standard protocol (Applied BioSystems, Inc). The primer sequences for the genes used in this study are listed in Supplemental Table 1.

Immunoblot.

Periosteal progenitors were seeded in 6-well plate treated with or without Plg for 24 hours. Culture medium was collected and concentrated by Amicon Ultra filters (UFC5003, Millipore). Bone fracture calluses were collected from $Plg^{+/+}$ and $Plg^{-/-}$ mice one week post fracture. Cells or tissue were lysed with a NP-40 buffer containing protease inhibitor cocktail. Proteins were resolved by 4–15% precast sodium dodecyl-sulfate polyacrylamide gel electrophoresis gel (Bio-Rad). After transferring, PVDF membranes were blotted with anti-GAPDH (1; 5000, cat#5174, Cell Signaling Technology), anti-Cyr61 (1:1,000, MAB4864, R&D systems) or anti-Integrins (1:1000, cat#4749, Cell Signaling Technology) antibodies. Proteins were detected with second antibodies specific for either rabbit or mouse IgG (Bio-Rad), followed by ECL development (RPN2232, GE Healthcare).

Statistics.

All data are visualized using box and whisker plots with the median represented by the line. All data points are displayed. Statistical significance was determined by unpaired Student's t-test using Prism 8 software (GraphPad Software, San Diego, CA, USA). For cell culture experiments, observations were repeated independently at least three times with a similar conclusion, and only data from a representative experiment are presented. Values of $p<0.05$ were considered significant.

Results

$Plg^{-/-}$ mice demonstrated decrements in cortical and trabecular bone properties

We first investigated the role of circulating Plg in normal bone metabolism. Plg deletion in $Plg^{-/-}$ mice was confirmed by ELSIA (Fig. S1A). Our data showed that femurs in $Plg^{-/-}$ mice were 12.2% shorter than those in $Plg^{+/+}$ siblings at 2 months of age (Fig. S2A). MicroCT analysis revealed that, $Plg^{-/-}$ mice had significantly reduced trabecular bone mass compared to $Plg^{+/+}$ mice (Fig. S2B), as evidenced by a drastically reduced BV/TV (55.3%) (Fig. S2C). This structural change was accompanied with a decrease of Tb.N (15%) and an increase of Tb.Sp (10%) as well as a trend of decrease of Tb. Th (11%). SMI score was also significantly increased by 21%, further indicating an impairment of structural integrity in $Plg^{-/-}$ trabecular bone.

Analyzing the cortical compartment revealed a similar detrimental effect on bone by Plg deficiency. The femoral shaft of $Plg^{-/-}$ mice was thinner and with reduced Ec.Pm (8%), Ps.Pm (12%), Ct.Th (12%), and Ct.Ar (20%) (Fig. 1A, B) than that in $Plg^{+/+}$ mice. The porosity of cortical bone was significantly increased by 23% and MOI, an indicator for bone resistance to bending, was significantly decreased by 20%. Moreover, cortical bone TMD declined by 5%. These results indicated that Plg is required for maintaining normal cortical bone structure.

Appositional bone growth is dependent on the new bone formation via periosteal mesenchymal progenitors and their offspring, periosteal osteoblasts. To understand the mechanism underlying the reduced cortical bone mass in $Plg^{-/-}$ mice, we collected periosteal cells from intact $Plg^{-/-}$ and $Plg^{+/+}$ tibiae, and seeded them for CFU-F analysis. CFU-F frequency and colony diameter were reduced by 18% and 13%, respectively, in $Plg^{-/-}$ mice compared to $Plg^{+/+}$ mice (Fig. 1C, D). Furthermore, when we used Plg-depleted culture medium for this assay, CFU-F colony formation was drastically reduced in periosteal cells from both $Plg^{+/+}$ and $Plg^{-/-}$ mice, suggesting that Plg is a critical factor for supporting the growth of periosteal mesenchymal progenitors. Note that Plg depletion in FBS was confirmed by ELSIA (Fig. S1B). A reduction in periosteal mesenchymal progenitor number is likely to be a major contributor to the cortical bone defects observed in Plg mice.

$Plg^{-/-}$ *mice exhibit delayed healing response after tibial fracture.*

Next we sought to elucidate the role of circulating Plg in bone regeneration after factures. Two-month-old $Plg^{-/-}$ and $Plg^{+/+}$ mice received closed, instrumented, and transverse fracture in their tibiae. Soon after fracture, $Plg^{+/+}$ mice had a small drop in body weight but quickly recovered after day 10 (Fig. S3). However, $Plg^{-/-}$ mice displayed a sustained loss in bone weight, implying an overall change in body metabolism after fracture. Weekly microCT scans after fracture showed that callus formation (TV) in $Plg^{+/+}$ mice reaches a peak at 10–14 days, gradually reducing in size at day 28, and achieved bone bridging and healing by day 42 (Fig. 2A, B, C). On the contrary, $Plg^{-/-}$ mice had much smaller calluses at days 5, 7, and 10. Their callus size finally reached a peak at day 28 and then declined at day 42. Bone mass in callus followed a same pattern, resulting similar bone volume fraction (BV/TV) between $Plg^{+/+}$ and $Plg^{-/-}$ mice at all time points. Different from fracture

healing in $Plg^{+/+}$ mice, we did not observe cortical bone bridging at the fracture site at day 42 in $Plg^{-/-}$ mice. Mechanical testing showed a remarkable reduction in peak load (51%), stiffness (31%), and energy to failure (71%) in $Plg^{-/-}$ mice compared to $Plg^{+/+}$ mice (Fig. 2D). Healing score was also significantly reduced in $Plg^{-/-}$ mice (Fig. 2E).

Next we performed histology to investigate the underlying cellular characteristics behind this impaired fracture healing. Long bone fractures are mostly repaired by endochondral ossification in which cartilage is first formed around the fracture gap and then replaced by bone formation [30]. As shown by Safranin O/Fast green staining in Fig. 3A, B, $Plg^{+/+}$ bones exhibited normal fracture repair processes with both callus and cartilage formation peaking around day 7–10 and bone formation peaking around day 14. Consistent with microCT results, callus formation in $Plg^{-/-}$ mice was significantly impeded during initial healing stages. This was reflected by 62% and 50% decreases of cartilage area at days 5 and 7, respectively. Bone area was also significantly reduced at all time points except day 28. In summary, these data demonstrated that Plg plays an important role in bone fracture healing, particularly at the early stage when chondrocytes are generated to form the soft callus.

The absence of Plg modifies the injury response of periosteal mesenchymal progenitors.

Bone repair after fracture starts with hematoma formation at the fracture site soon followed by periosteal thickening along the nearby bone surfaces. At this early stage, periosteal mesenchymal progenitors undergo rapid proliferation. Later, the inner cells of the thickened periosteum (close to the facture line) differentiate into chondrocytes and cells in the less thickened periosteum (at the region away from the fracture line) preferentially differentiate into osteoblasts [27,31].

Within this paradigm, we observed that the thickness and area of the expanded periosteum at day 3 post fracture was significantly reduced in $Plg^{-/-}$ mice, by 27% and 22%, respectively, when compared to those in $Plg^{+/+}$ mice (Fig. 4A, B). Furthermore, EdU incorporation assay revealed that the percentage of proliferative cells within the expanding periosteum was significantly decreased from 32% in $Plg^{+/+}$ mice to 26% in $Plg^{-/-}$ mice.

To test whether Plg regulates chondrogenic and osteoblastic differentiation of periosteal mesenchymal progenitors, we first compared the differentiation ability of periosteal mesenchymal progenitors from $Plg^{+/+}$ and $Plg^{-/-}$ mice; no significant difference was found. In particular, under chondrogenic differentiation conditions, $Plg^{-/-}$ cells developed a pellet with size and the GAG content that could not be distinguished from $Plg^{+/+}$ cells (Fig. 5A, B). Consistent with this, RNA analysis revealed equivalent up-regulation of chondrogenic marker gene expression (*Sox9, Acan, Col2α1,* and *Col10α1*) in $Plg^{+/+}$ and $Plg^{-/-}$ cells (Fig. 5C). Alizarin Red staining (Fig. 5D) and RNA analysis of gene expression of osteoblastic transcription factors (*Sp7*) and markers (*Ibsp* and *Bglap2*) (Fig. 5E) also showed similar results when tested for osteogenic differentiation. While the up-regulation of *Runx2* expression in $Plg^{-/-}$ cells was not as high as that in $Plg^{+/+}$ cells, we still believe that there is no intrinsic difference in the differentiation of $Plg^{+/+}$ and $Plg^{-/-}$ progenitors.

Since Plg is secreted exclusively by liver cells and then circulates in the blood at a high concentration [32], we tested whether environmental Plg would affect osteogenic

differentiation using normal or Plg-depleted FBS in culture. Depletion of Plg in the medium almost completely abolished the mineralization of both $Plg^{+/+}$ and $Plg^{-/-}$ cells in otherwise osteogenic culture and remarkably reduced the expression of *Runx2, Ibsp,* and *Sp7* in both $Plg^{+/+}$ and $Plg^{-/-}$ cells. Considering reduced bone mass phenotype in Plg KO mice (Fig 1, and S2), these data suggested that Plg is a critical factor for osteoblast differentiation in bone metabolism and regeneration. Since chondrogenic differentiation medium does not contain serum (which would typically be the source of Plg), we conclude that chondrogenic differentiation does not require Plg contribution.

Cartilage-to-bone remodeling after fracture in $Plg^{-/-}$ mice is moderately delayed.

A previous study reported that bone healing in $Plg^{-/-}$ mice is completely blunted at the remodeling step that converts cartilage matrix into bone due to the blockage effect of fibrin matrix at the chondro-osseous junction (COJ) [8]. However, our radiographic and histologic examination demonstrated that bone healing could pass through this stage in $Plg^{-/-}$ mice. To investigate this further, we performed vessel staining at day 10 post fracture, when remodeling is at its peak, using Emcn as a vessel marker (Fig. 6A, B). Quantification of vessel number and length along the chondro-osseous junction (COJ) revealed a modest decline in $Plg^{-/-}$ mice compared to $Plg^{+/+}$ mice (23% and 27%, respectively, Fig. 6C). In addition, TRAP staining showed that osteoclasts in the callus are also reduced in number (Fig. S4). Since vessel invasion-it brings in osteoprogenitor and osteoclasts for bone formation and cartilage matrix degradation-is a good indicator for cartilage-to-bone remodeling, our data indicated that this remodeling process, while still functional in $Plg^{-/-}$ mice, is delayed. IHC staining revealed that at the same time, fibrin matrix is still present at the COJ and bone marrow at day 10 (Fig. 6D). At the late bone remodeling stage, fibrin staining persisted at the fracture gap (Fig. 6E,F), indicating that the presence of fibrin due to the loss of Plg does not block the progression of cartilage-to-bone remodeling during fracture repair.

Plg stimulates proliferation, survival and migration of periosteal mesenchymal progenitors

Plg has been shown essential for cell proliferation and migration [6,9,33]. However, whether Plg regulates cell function of periosteal progenitors remains unknown. To test whether Plg plays a role in cell behavior of periosteal mesenchymal progenitors, we harvested periosteal mesenchymal progenitors from healthy $Plg^{+/+}$ mice and evaluated cell proliferation and survival under hypoxia condition to mimic the ischemic hypoxic environment at the fracture site. Our data showed that cell growth is inhibited in the control group by hypoxia (5% oxygen); however, the proliferation of progenitors was rapidly increased by Plg treatment, especially at 24h (Fig. 7A). Meanwhile, under severe hypoxia (2% oxygen), cells were undergoing apoptosis as analyzed by flow cytometry; however, Plg treatment significantly protected cell apoptosis at either low dose (PlgL) or high dose (PlgH) compare to controls (Fig. 7B,C). Furthermore, we evaluated whether Plg is required for migration of periosteal mesenchymal progenitors. Progenitors were collected and subjected to migration assay using transwell system. Our data (Fig. 7D) showed that Plg robustly increased cell migration (10-fold) compared to the control group. Taken together, Plg promoted proliferation, survival as well as migration of periosteal progenitors which may contribute to bone repair and regeneration.

Plg activates Cyr61 by cleavage to promote periosteal mesenchymal progenitor proliferation and migration.

Cyr61 is a matrix-associated protein, which is critical for bone regeneration and bone repair[34,35]. After secretion, Cyr61 is deposited in extracellular matrix and has to be released by proteolysis to act on cells [36,37]. It is reported that Plg could activate Cyr61 by cleaving it into a truncated form in fibroblasts and tumor cells [38,39]. Therefore, we investigated whether Plg is able to activate Cyr61 in periosteal progenitors to impact cell function. Progenitors were treated with Plg and cell lysate and culture medium were subjected to immunoblot assay. Remarkably, after Plg treatment, the truncated form of Cyr61 was detected in culture media (Fig. 8A); however, full length Cyr61 was much less detectable in cell lysates with Plg treatment, indicating more Cyr61 were cleaved into soluble form by Plg and released to the culture medium. We also analyzed fracture calluses collected from $Plg^{+/+}$ and $Plg^{-/-}$ mice (Fig. 8B). Interestingly, truncated Cyr61 was only detected in $Plg^{+/+}$ but not $Plg^{-/-}$ mice, indicating Plg activates Cyr61 *in vivo*. Furthermore, we tested the role of Cyr61 in Plg-mediated viability and motility of progenitors. Our data showed that a neutralizing antibody to Cyr61 significantly inhibited Plg-stimulated cell proliferation (Fig. 8C) and almost completely inhibited Plg-induced cell migration (Fig. 8D, E). These results strongly suggest that Plg can regulate periosteal progenitor proliferation and migration through activation of Cyr61.

Cyr61 is known to regulate cell proliferation, adhesion and migration by binding to Integrins, including Integrin αvβ1, αvβ3, αvβ5 [40–42]. Cyr61 can also trigger a 'Cyr61-Integrin autocrine loop' to increase Integrin expression and contributes to tumor growth and angiogenesis [43]. To test which Integrin is likely involved in Plg/Cyr61 regulated cell function, periosteal mesenchymal progenitors were treated with Plg or Plg plus Cyr61 antibody under normoxia and hypoxia, and Integrin expression was measured. Immunoblotting data (Fig. 9A, B) showed that hypoxia increased amount of several Integrins in periosteal progenitors; however, only Integrin β5 was increased by Plg under hypoxia condition. Further, Cyr61 neutralizing antibodies inhibited Plg-induced Integrin β5 expression, indicating that Plg may regulate cell proliferation and migration through Cyr61-Integrin β5 interaction. To test whether Integrin β5 is involved in Plg-regulated cell migration, we knocked down Integrin β5 by siRNA in periosteal progenitors and cell migration under hypoxia was tested. Immunoblotting data indicated that Integrin β5 knockdown by siRNA was efficient on progenitors (Fig. 9C). Interestingly, Plg-regulated cell migration was significantly reduced by Integrin β5 knockdown (Fig. 9D,E), indicating that Plg/Cyr61 may mediate progenitor migration through Integrin β5.

Discussion

Plg has been implicated in regulation of hematopoietic stem cell mobilization during cardiac repair [6]; however, the role of Plg in periosteal mesenchymal progenitors during bone development and repair, while hypothetically compelling, has not been clearly investigated. Here, our data demonstrate that Plg is critical for developing the structural integrity of trabecular bone as well as the morphology of cortical bone and substantially contributes to healing after traumatic long-bone fracture in mice. Through in vivo and ex

vivo experiments, our studies further suggest that Plg stimulates periosteal mesenchymal progenitor proliferation and migration. Mechanistic studies reveal that Plg can cleave and activate Cyr61, a matrix-associated growth factor that is secreted by progenitors and essential for their proliferation and migration, which consequently contributes to fracture healing.

Local mesenchymal stem cells (MSCs) from the periosteum are the primary cell source for bone repair after fracture [3,4]. During fracture healing, periosteal progenitors undergo proliferation, migration to the cartilage callus, and differentiation into cartilage-forming chondrocytes and bone-forming osteoblasts to promote bone repair [31,44]. Our data shows an essential role of Plg in regulation of the proliferation, migration and survival of periosteal progenitors during fracture healing. $Plg^{-/-}$ mice exhibit reduced trabecular bone and cortical bone mass, indicating that Plg is critical for bone metabolism during development and base-line physiological conditions. Interestingly, although there was no intrinsic difference in chondrogenic and osteogenic differentiation in periosteal mesenchymal progenitors isolated from $Plg^{+/+}$ and $Plg^{-/-}$ mice, osteogenic differentiation was completely abrogated in medium depleted of Plg. This suggested that Plg is critical for osteogenic periosteal progenitor differentiation, the loss of which may partially contribute to bone mass loss in $Plg^{-/-}$ mice. More direct in vivo evidence is needed to draw specific conclusions regarding mechanisms underlying Plg-regulated osteognic differentiation and will need to be further investigated.

In addition to their regenerative potential, mesenchymal progenitors can also produce secretory factors that promote tissue repair and modulate immune response [45–47]. Cyr61 is a matrix-associated growth factor secreted by many types of cells including endothelial cells, fibroblasts, and MSCs [48–50]. Cyr61 promotes cell migration and proliferation and plays an important role in angiogenesis, fibrosis and tumor metastasis [37,51–53]. Our data reveals that Cyr61, secreted by periosteal mesenchymal cells, can be activated by Plg to release a soluble, active form in culture. Cyr61 neutralization abrogates Plg-induced proliferation and migration of periosteal progenitors in vitro. Moreover, Plg cleaves Cyr61 in mouse fracture calluses, suggesting a new mechanism for Plg-inducible autocrine activity to stimulate periosteal mesenchymal progenitors during fracture healing. Cyr61 is well known for its pro-angiogenic property through Integrin binding to induce endothelial cell proliferation and migration [41,51]. Consistent with this role, our data show that Plg deletion reduces vessel density, suggesting a possible paracrine effect of periosteal progenitors through Plg/Cyr61 in angiogenesis during bone repair. We speculate that Plg/Cyr61-mediated angiogenesis may represent a previously undescribed mechanism regulating bone repair.

Consistent with our results, previous studies using drill hole and femoral surgical fracture models have shown that bone repair is impaired in $Plg^{-/-}$ mice. However, these studies suggested different mechanisms mediated through 1) down-regulation of VEGF-A and TGF-β expression, angiogenesis, and macrophage accumulation in a drill hole model [8] and 2) Plm deficiency-induced fibrin accumulation that blocks facture neovascularization and cartilaginous remodeling in an open-surgical femoral fracture model [21]. Notably, our data with a closed traumatic femoral fracture model shows a moderate reduction (~20%) in neo-vessel numbers along the COJ remodeling region. While fibrin exists abundantly

in the fracture callus up to day 28 post fracture, the cartilage to bone remodeling in $Plg^{-/-}$ mice still proceeds. The major morphologic deficiency in bone repair in $Plg^{-/-}$ mice seems to be that periosteal expansion is attenuated after fracture, consistent with less periosteal mesenchymal progenitors detected in $Plg^{-/-}$ mice. Interestingly, while Plg does not specifically affect the chondrogenic differentiation of progenitors, Plg is critical for MSC proliferation and survival, e.g., expansion of those progenitors (based on CFU-F assay) relies on the presence of Plg in the medium, suggesting that the reduced callus volume in $Plg^{-/-}$ mice is likely due to a diminished proliferative response of periosteal progenitors. Collectively, our results indicated that impaired periosteal progenitor function, but not reduced angiogenesis caused by fibrin deposition, represents a major mechanism underlying the deficient fracture repair in $Plg^{-/-}$ mice.

In summary, our study reveals an alternative role of Plg in regulation of periosteal progenitor functions and fracture healing, identifying a previously uncharacterized autocrine/paracrine mechanism. Biologically, this mechanism provides a compelling therapeutic target as a rate limiting step in problem fracture healing (eg those in the aged) includes an appropriate MSC response. Clinically, this protein provides a compelling therapeutic target as thrombolytic treatment with Plg is already being utilized safely including in the traumatically injured; the ability to stimulate Plg activity locally and temporally would further enhance efficacy and safety. Therefore, the targeting of Plg represents as a novel, rational and safe strategy for enhancing bone repair and regeneration.

Supplementary Material

Refer to Web version on PubMed Central for supplementary material.

Acknowledgments

This study was in part supported by AHA Grant 17GRNT33650029 (to Y.G.), NIH grants R01DK095803 (to L.Q.), and P30AR069619 (to Penn Center for Musculoskeletal Disorders).

Reference

1. Marzona L, Pavolini B. Play and players in bone fracture healing match. Clin Cases Miner Bone Metab. 2009;6(2):159–62. [PubMed: 22461167]
2. Claes L, Recknagel S, Ignatius A. Fracture healing under healthy and inflammatory conditions. Nat Rev Rheumatol. 2012;8(3):133–43. [PubMed: 22293759]
3. Bragdon BC, Bahney CS. Origin of Reparative Stem Cells in Fracture Healing. Curr Osteoporos Rep. 2018;16(4):490–503. [PubMed: 29959723]
4. Knight MN, Hankenson KD. Mesenchymal Stem Cells in Bone Regeneration. Adv Wound Care (New Rochelle). 2013;2(6):306–16. [PubMed: 24527352]
5. Romer J, Bugge TH, Pyke C, et al. Impaired wound healing in mice with a disrupted plasminogen gene. Nat Med. 1996;2(3):287–92. [PubMed: 8612226]
6. Gong Y, Zhao Y, Li Y, Fan Y, Hoover-Plow J. Plasminogen regulates cardiac repair after myocardial infarction through its noncanonical function in stem cell homing to the infarcted heart. J Am Coll Cardiol. 2014;63(25 Pt A):2862–72. [PubMed: 24681141]
7. Kawao N, Nagai N, Okada K, Okumoto K, Ueshima S, Matsuo O. Role of plasminogen in macrophage accumulation during liver repair. Thromb Res. 2010;125(5):e214–21. [PubMed: 20064655]

8. Kawao N, Tamura Y, Okumoto K, et al. Plasminogen plays a crucial role in bone repair. J Bone Miner Res. 2013;28(7):1561–74. [PubMed: 23456978]
9. Gong Y, Hart E, Shchurin A, Hoover-Plow J. Inflammatory macrophage migration requires MMP-9 activation by plasminogen in mice. J Clin Invest. 2008;118(9):3012–24. [PubMed: 18677407]
10. Kenagy RD, Vergel S, Mattsson E, Bendeck M, Reidy MA, Clowes AW. The role of plasminogen, plasminogen activators, and matrix metalloproteinases in primate arterial smooth muscle cell migration. Arterioscler Thromb Vasc Biol. 1996;16(11):1373–82. [PubMed: 8911276]
11. Sleight P Thrombolysis: state of the art. Eur Heart J. 1993;14 Suppl G:41–7.
12. investigators G. An international randomized trial comparing four thrombolytic strategies for acute myocardial infarction. N Engl J Med. 1993;329(10):673–82. [PubMed: 8204123]
13. Neffendorf JE, Kirthi V, Pringle E, Jackson TL. Ocriplasmin for symptomatic vitreomacular adhesion. Cochrane Database Syst Rev. 2017;10:CD011874. [PubMed: 29040800]
14. Dugel PU, Tolentino M, Feiner L, Kozma P, Leroy A. Results of the 2-Year Ocriplasmin for Treatment for Symptomatic Vitreomacular Adhesion Including Macular Hole (OASIS) Randomized Trial. Ophthalmology. 2016;123(10):2232–47. [PubMed: 27499517]
15. Everts V, Daci E, Tigchelaar-Gutter W, et al. Plasminogen activators are involved in the degradation of bone by osteoclasts. Bone. 2008;43(5):915–20. [PubMed: 18691680]
16. Daci E, Everts V, Torrekens S, et al. Increased bone formation in mice lacking plasminogen activators. J Bone Miner Res. 2003;18(7):1167–76. [PubMed: 12854826]
17. Kawao N, Tamura Y, Okumoto K, et al. Tissue-type plasminogen activator deficiency delays bone repair: roles of osteoblastic proliferation and vascular endothelial growth factor. Am J Physiol Endocrinol Metab. 2014;307(3):E278–88. [PubMed: 24918201]
18. Daci E, Verstuyf A, Moermans K, Bouillon R, Carmeliet G. Mice lacking the plasminogen activator inhibitor 1 are protected from trabecular bone loss induced by estrogen deficiency. J Bone Miner Res. 2000;15(8):1510–6. [PubMed: 10934649]
19. Rundle CH, Wang X, Wergedal JE, Mohan S, Lau KH. Fracture healing in mice deficient in plasminogen activator inhibitor-1. Calcif Tissue Int. 2008;83(4):276–84. [PubMed: 18820962]
20. Kanno Y, Ishisaki A, Kawashita E, et al. Plasminogen/plasmin modulates bone metabolism by regulating the osteoblast and osteoclast function. J Biol Chem. 2011;286(11):8952–60. doi: 10.1074/jbc.M110.152181. Epub 2011 Jan 14. [PubMed: 21239499]
21. Yuasa M, Mignemi NA, Nyman JS, et al. Fibrinolysis is essential for fracture repair and prevention of heterotopic ossification. J Clin Invest. 2015;125(8):3117–31. [PubMed: 26214526]
22. Carmeliet P, Moons L, Lijnen R, et al. Urokinase-generated plasmin activates matrix metalloproteinases during aneurysm formation. Nat Genet. 1997;17(4):439–44. [PubMed: 9398846]
23. Yee JA, Yan L, Dominguez JC, Allan EH, Martin TJ. Plasminogen-dependent activation of latent transforming growth factor beta (TGF beta) by growing cultures of osteoblast-like cells. J Cell Physiol. 1993;157(3):528–34. [PubMed: 8253864]
24. Whitelock JM, Murdoch AD, Iozzo RV, Underwood PA. The degradation of human endothelial cell-derived perlecan and release of bound basic fibroblast growth factor by stromelysin, collagenase, plasmin, and heparanases. J Biol Chem. 1996;271(17):10079–86. [PubMed: 8626565]
25. Matsuoka H, Sisson TH, Nishiuma T, Simon RH. Plasminogen-mediated activation and release of hepatocyte growth factor from extracellular matrix. American journal of respiratory cell and molecular biology. 2006;35(6):705–13. [PubMed: 16840775]
26. Ploplis VA, French EL, Carmeliet P, Collen D, Plow EF. Plasminogen deficiency differentially affects recruitment of inflammatory cell populations in mice. Blood. 1998;91(6):2005–9. [PubMed: 9490683]
27. Wang L, Tower RJ, Chandra A, et al. Periosteal Mesenchymal Progenitor Dysfunction and Extraskeletally-Derived Fibrosis Contribute to Atrophic Fracture Nonunion. J Bone Miner Res. 2019;34(3):520–32. [PubMed: 30602062]
28. Warden SJ, Komatsu DE, Rydberg J, Bond JL, Hassett SM. Recombinant human parathyroid hormone (PTH 1–34) and low-intensity pulsed ultrasound have contrasting additive effects during fracture healing. Bone. 2009;44(3):485–94. [PubMed: 19071238]

29. Deutsch DG, Mertz ET. Plasminogen: purification from human plasma by affinity chromatography. Science. 1970;170(3962):1095–6. [PubMed: 5475635]
30. Marsell R, Einhorn TA. The biology of fracture healing. Injury. 2011;42(6):551–5. [PubMed: 21489527]
31. Wang T, Zhang X, Bikle DD. Osteogenic Differentiation of Periosteal Cells During Fracture Healing. J Cell Physiol. 2017;232(5):913–21. [PubMed: 27731505]
32. Raum D, Marcus D, Alper CA, Levey R, Taylor PD, Starzl TE. Synthesis of human plasminogen by the liver. Science. 1980;208(4447):1036–7. [PubMed: 6990488]
33. Hayashi M, Tamura Y, Dohmae N, Kojima S, Shimonaka M. Plasminogen N-terminal activation peptide modulates the activity of angiostatin-related peptides on endothelial cell proliferation and migration. Biochem Biophys Res Commun. 2008;369(2):635–40. [PubMed: 18294956]
34. Zhao G, Huang BL, Rigueur D, et al. CYR61/CCN1 Regulates Sclerostin Levels and Bone Maintenance. J Bone Miner Res. 2018;33(6):1076–89. [PubMed: 29351359]
35. Liu H, Peng F, Liu Z, et al. CYR61/CCN1 stimulates proliferation and differentiation of osteoblasts in vitro and contributes to bone remodeling in vivo in myeloma bone disease. Int J Oncol. 2017;50(2):631–9. [PubMed: 28035364]
36. Kireeva ML, Mo FE, Yang GP, Lau LF. Cyr61, a product of a growth factor-inducible immediate-early gene, promotes cell proliferation, migration, and adhesion. Molecular and cellular biology. 1996;16(4):1326–34. [PubMed: 8657105]
37. Babic AM, Kireeva ML, Kolesnikova TV, Lau LF. CYR61, a product of a growth factor-inducible immediate early gene, promotes angiogenesis and tumor growth. Proc Natl Acad Sci U S A. 1998;95(11):6355–60. [PubMed: 9600969]
38. Mandal SK, Rao LV, Tran TT, Pendurthi UR. A novel mechanism of plasmin-induced mitogenesis in fibroblasts. J Thromb Haemost. 2005;3(1):163–9. [PubMed: 15634280]
39. Pendurthi UR, Tran TT, Post M, Rao LV. Proteolysis of CCN1 by plasmin: functional implications. Cancer Res. 2005;65(21):9705–11. [PubMed: 16266990]
40. Monnier Y, Farmer P, Bieler G, et al. CYR61 and alphaVbeta5 integrin cooperate to promote invasion and metastasis of tumors growing in preirradiated stroma. Cancer Res. 2008;68(18):7323–31. [PubMed: 18794119]
41. Leu SJ, Lam SC, Lau LF. Pro-angiogenic activities of CYR61 (CCN1) mediated through integrins alphavbeta3 and alpha6beta1 in human umbilical vein endothelial cells. J Biol Chem. 2002;277(48):46248–55. [PubMed: 12364323]
42. Lau LF. Cell surface receptors for CCN proteins. J Cell Commun Signal. 2016;10(2):121–7. [PubMed: 27098435]
43. Menendez JA, Vellon L, Mehmi I, Teng PK, Griggs DW, Lupu R. A novel CYR61-triggered 'CYR61-alphavbeta3 integrin loop' regulates breast cancer cell survival and chemosensitivity through activation of ERK1/ERK2 MAPK signaling pathway. Oncogene. 2005;24(5):761–79. [PubMed: 15592521]
44. Duchamp de Lageneste O, Julien A, Abou-Khalil R, et al. Periosteum contains skeletal stem cells with high bone regenerative potential controlled by Periostin. Nature communications. 2018;9(1):773.
45. Fan XL, Zhang Y, Li X, Fu QL. Mechanisms underlying the protective effects of mesenchymal stem cell-based therapy. Cell Mol Life Sci. 2020:In press.
46. Ranganath SH, Levy O, Inamdar MS, Karp JM. Harnessing the mesenchymal stem cell secretome for the treatment of cardiovascular disease. Cell Stem Cell. 2012;10(3):244–58. [PubMed: 22385653]
47. Sun DZ, Abelson B, Babbar P, Damaser MS. Harnessing the mesenchymal stem cell secretome for regenerative urology. Nat Rev Urol. 2019;16(6):363–75. [PubMed: 30923338]
48. Brigstock DR. Regulation of angiogenesis and endothelial cell function by connective tissue growth factor (CTGF) and cysteine-rich 61 (CYR61). Angiogenesis. 2002;5(3):153–65. [PubMed: 12831056]
49. Estrada R, Li N, Sarojini H, An J, Lee MJ, Wang E. Secretome from mesenchymal stem cells induces angiogenesis via Cyr61. J Cell Physiol. 2009;219(3):563–71. [PubMed: 19170074]

50. Pendurthi UR, Ngyuen M, Andrade-Gordon P, Petersen LC, Rao LV. Plasmin induces Cyr61 gene expression in fibroblasts via protease-activated receptor-1 and p44/42 mitogen-activated protein kinase-dependent signaling pathway. Arterioscler Thromb Vasc Biol. 2002;22(9):1421–6. [PubMed: 12231560]

51. Chen N, Leu SJ, Todorovic V, Lam SC, Lau LF. Identification of a novel integrin alphavbeta3 binding site in CCN1 (CYR61) critical for pro-angiogenic activities in vascular endothelial cells. J Biol Chem. 2004;279(42):44166–76. [PubMed: 15308622]

52. Jun JI, Lau LF. The matricellular protein CCN1 induces fibroblast senescence and restricts fibrosis in cutaneous wound healing. Nat Cell Biol. 2010;12(7):676–85. [PubMed: 20526329]

53. Li J, Ye L, Owen S, Weeks HP, Zhang Z, Jiang WG. Emerging role of CCN family proteins in tumorigenesis and cancer metastasis (Review). Int J Mol Med. 2015;36(6):1451–63. [PubMed: 26498181]

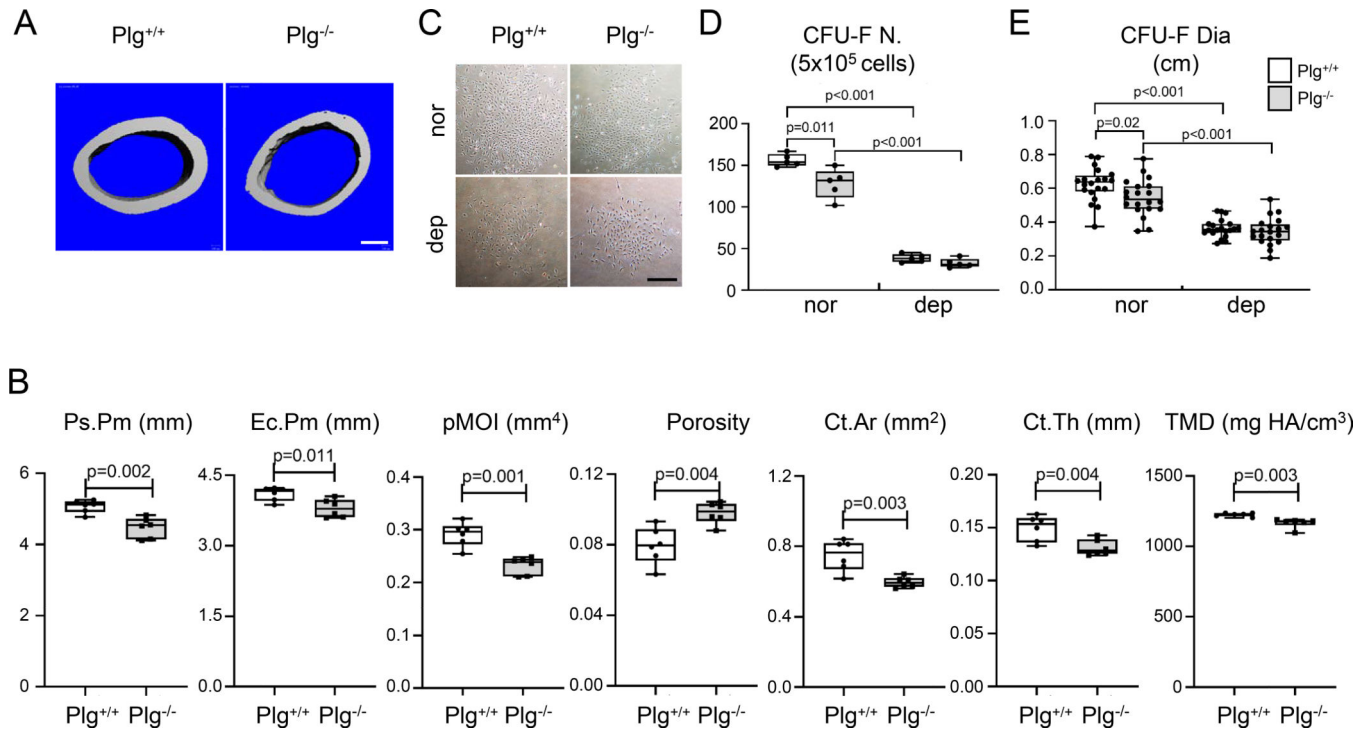

Figure 1. Plg deficiency causes cortical bone loss in mouse femur.

(A) 3D reconstructed microCT images of cortical bone from 2-month-old $Plg^{+/+}$ and $Plg^{-/-}$ femurs. Scale bar = 300 μm. (B) MicroCT measurement of femoral cortical bone structural parameters. Scale bar = 200 μm. (C) Images of CFU-F colonies of the periosteal mesenchymal cells derived from $Plg^{+/+}$ and $Plg^{-/-}$ mouse femurs cultured in medium containing normal (nor) or Plg depleted FBS (dep) for 10 days. (D) CFU-F colony number (No) and diameter (Dia) were quantified. n = 6 mice/group.

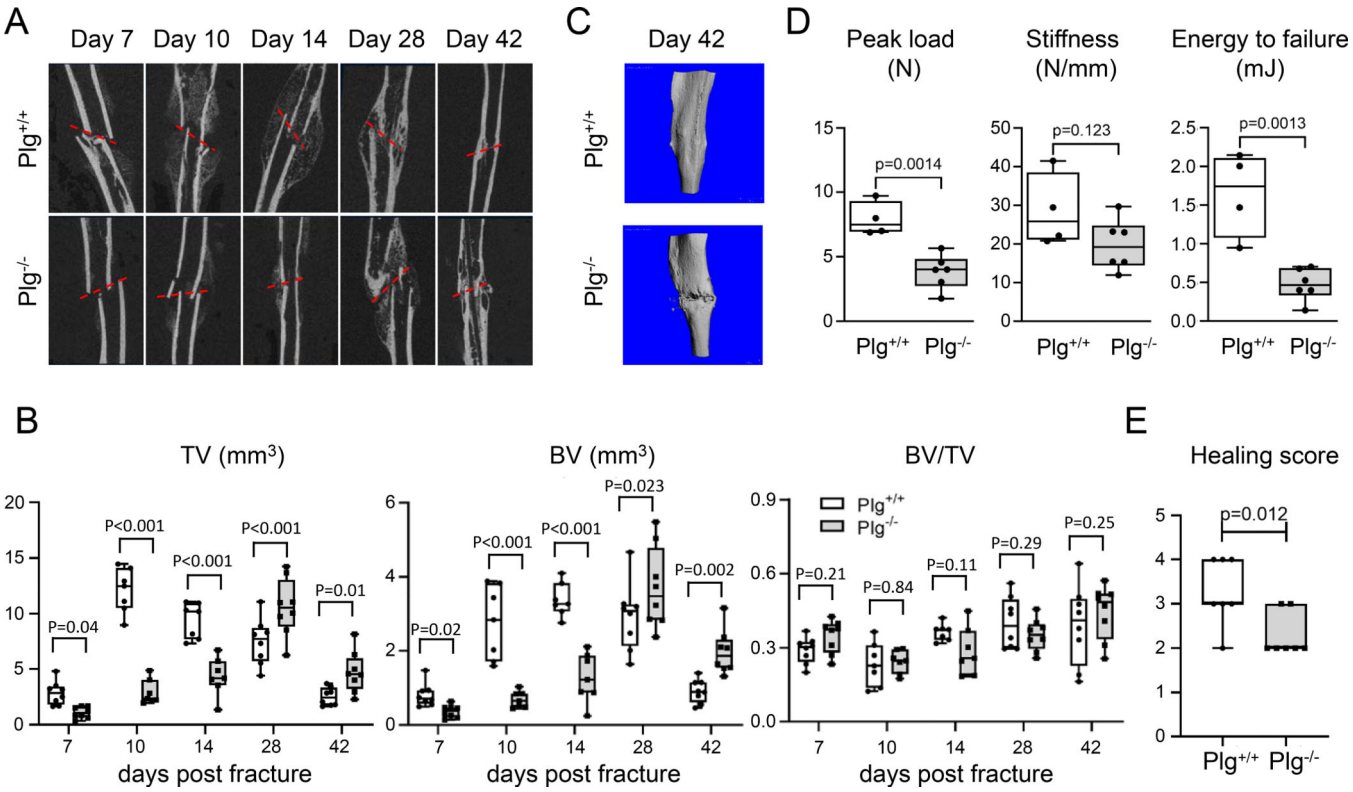

Figure 2. Plasminogen deficient mice have impaired fracture healing.

(A) Representative 2D microCT images of fracture calluses at 7, 10, 14, 28 and 42 days post fracture. Dashed red lines depict the fracture lines. Scale bar = 1 mm. (B) Callus tissue volume (TV), bone volume (BV), and bone volume fraction (BV/TV) of fracture calluses post fracture were measured. n = 7–8 mice/group. (C) 3D reconstructed tibias at 42 days post fracture. Scale bar = 1 mm. (D) Three-point bending test was performed on tibiae at 42 days post fracture. n = 4–6 mice/group. (E) Fracture healing scores were quantified on tibiae at 42 days post fracture. n = 7 mice/group.

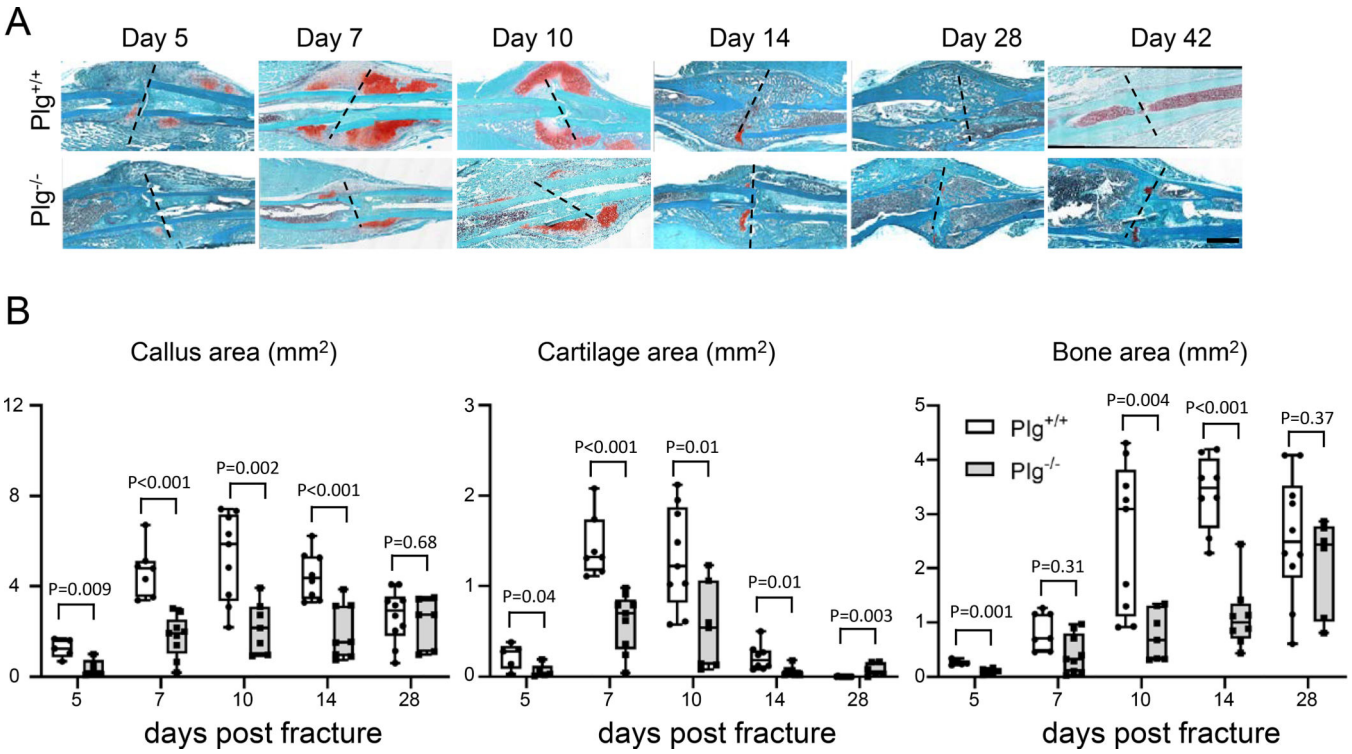

Figure 3. Fracture healing is impaired in Plasminogen deficient mice.

(A) Representative Safranin O/Fast green staining images of fracture calluses at 5, 7, 10, 14, 28 and 42 days post fracture. Dashed black lines depict the fracture lines. Scale bar =1 mm. (B) Callus area, cartilage area, and bone area were measured post fracture. n=5–10 mice/group.

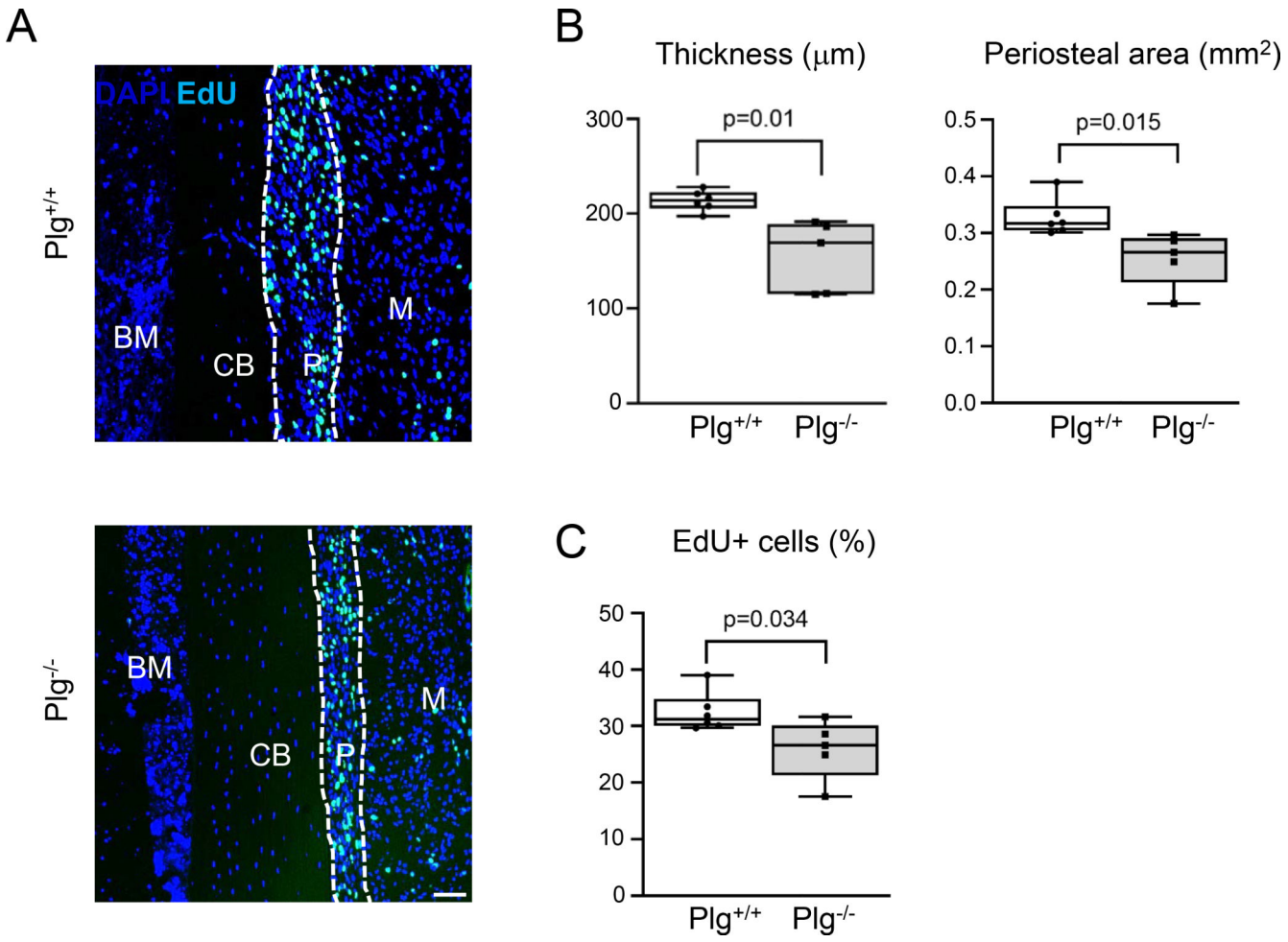

Figure 4. The periosteum responses toward fracture are reduced in Plg-deficient mice.

(A) EdU staining of expanded periosteum (outlined by white lines) at 3 days post fracture. CB: cortical bone; P, periosteum; M, muscle; BM, bone marrow. Green, EdU; blue, DAPI. Scale bar = 100 μm. (B, C) Thickness and area of expanded periosteum, and the percentage of EdU+ cells within all DAPI+ cells in the expanded periosteum were quantified. n=5–6 mice/group.

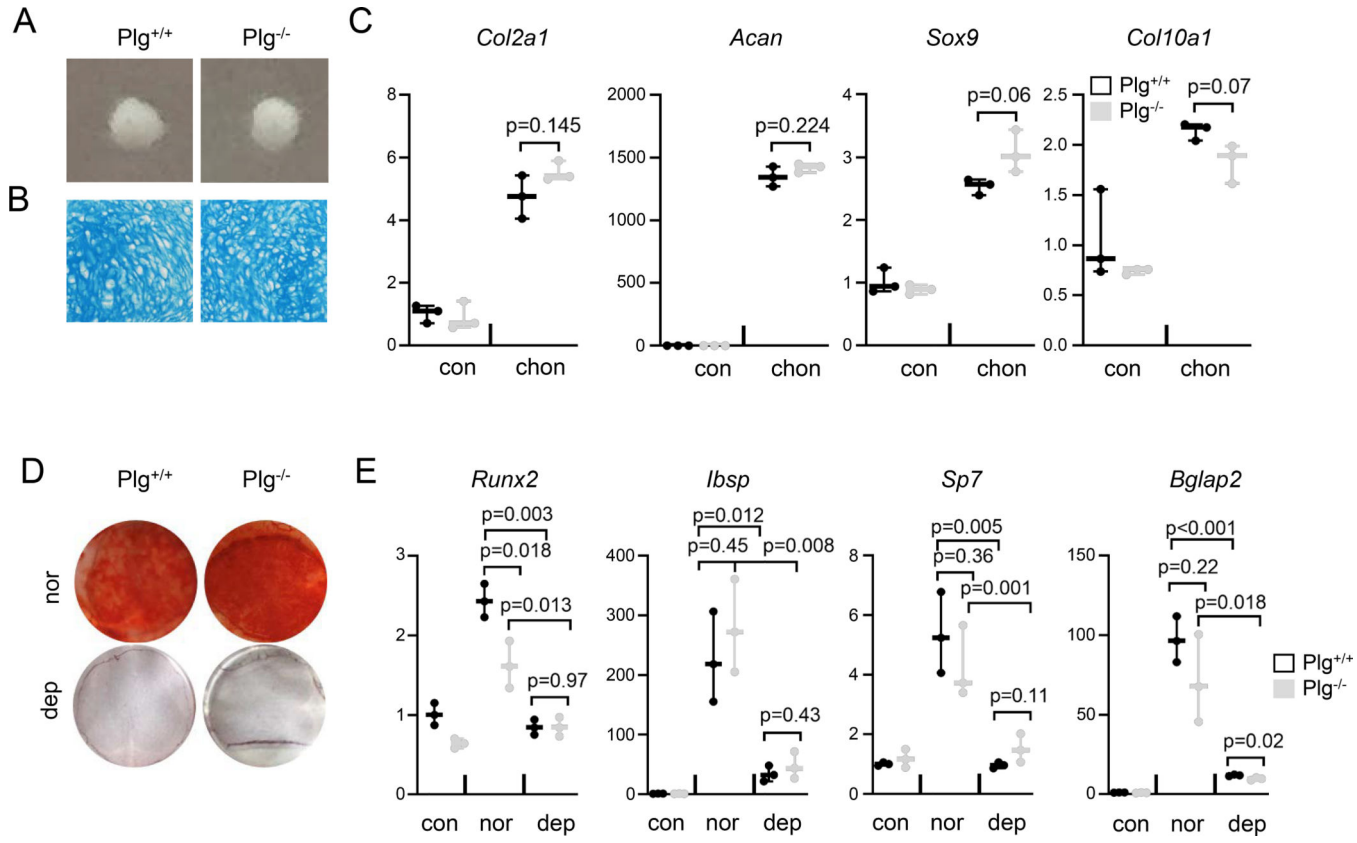

Figure 5. Plg is critical for the differentiation of periosteal progenitor cells.

(A) Images of cell pellets formed by periosteal mesenchymal progenitors from $Plg^{+/+}$ and $Plg^{-/-}$ mice after culturing in chondrogenic medium for 3 weeks. (B) Alcian blue staining of sections from chondrogenic cell pellets. (C) Real-time RT-PCR analysis of chondrogenic marker gene expression in cell pellets harvested after 2 weeks of culture in chondrogenic medium. (D) Alizarin red staining of periosteal mesenchymal progenitors from $Plg^{+/+}$ and $Plg^{-/-}$ mice after culturing in osteogenic medium with normal FBS (nor) or Plasminogen-depleted FBS (dep) for 2 weeks. (E) Real-time RT-PCR analysis of osteogenic marker gene expression in cells harvested after 2 weeks of culture in osteogenic medium.

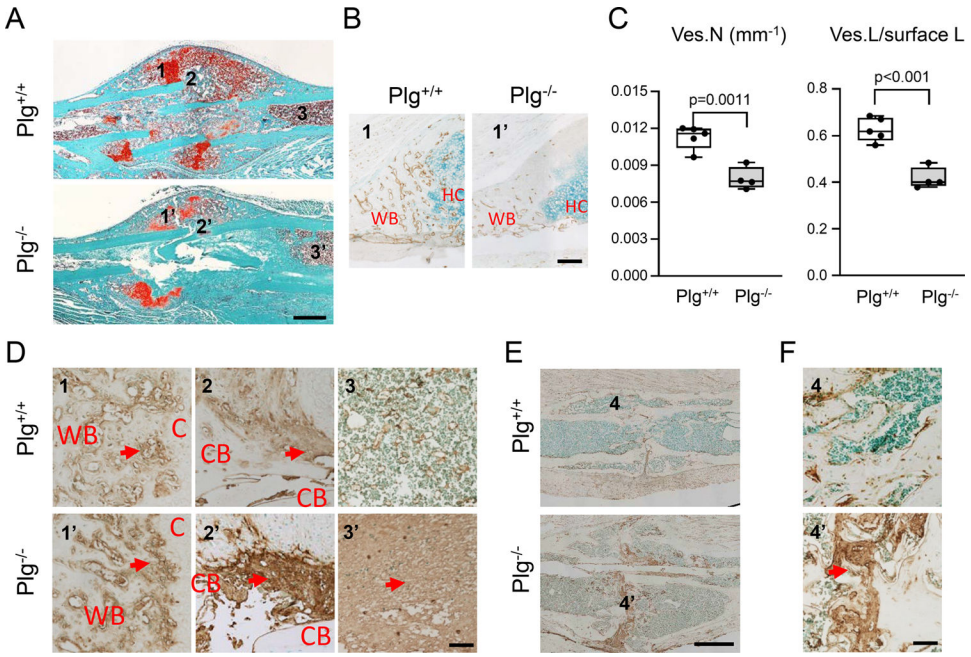

Figure 6. Persistence of blood clot within the fracture callus impairs fracture healing in Plg-deficient mice.

(A) Representative Safranin O/Fast green staining images of fracture calluses at 10 days post fracture. Scale bar = 1 mm. (B) Endomucin staining images of region 1 (COJ). WB, woven bone; HC, hypertrophic chondrocyte. Scale bar = 250 μm. (C) Quantification of vessel number (Ves.N) and the percentage of vessel length in the COJ surface length (Ves.L/surface L). (D) Fibrin staining images of regions 1 (COJ), 2 (fracture site), 3 (bone marrow). Red arrows point to positive staining. CB, cortical bone; C, cartilage. Scale bar = 100 μm. (E) Representative fibrin staining images of fracture calluses at 28 days post fracture. Scale bar = 1 mm. (F) Fibrin staining images of region 4 (fracture site). Red arrow points to positive staining. Scale bar = 100 μm. n = 4 mice/group.

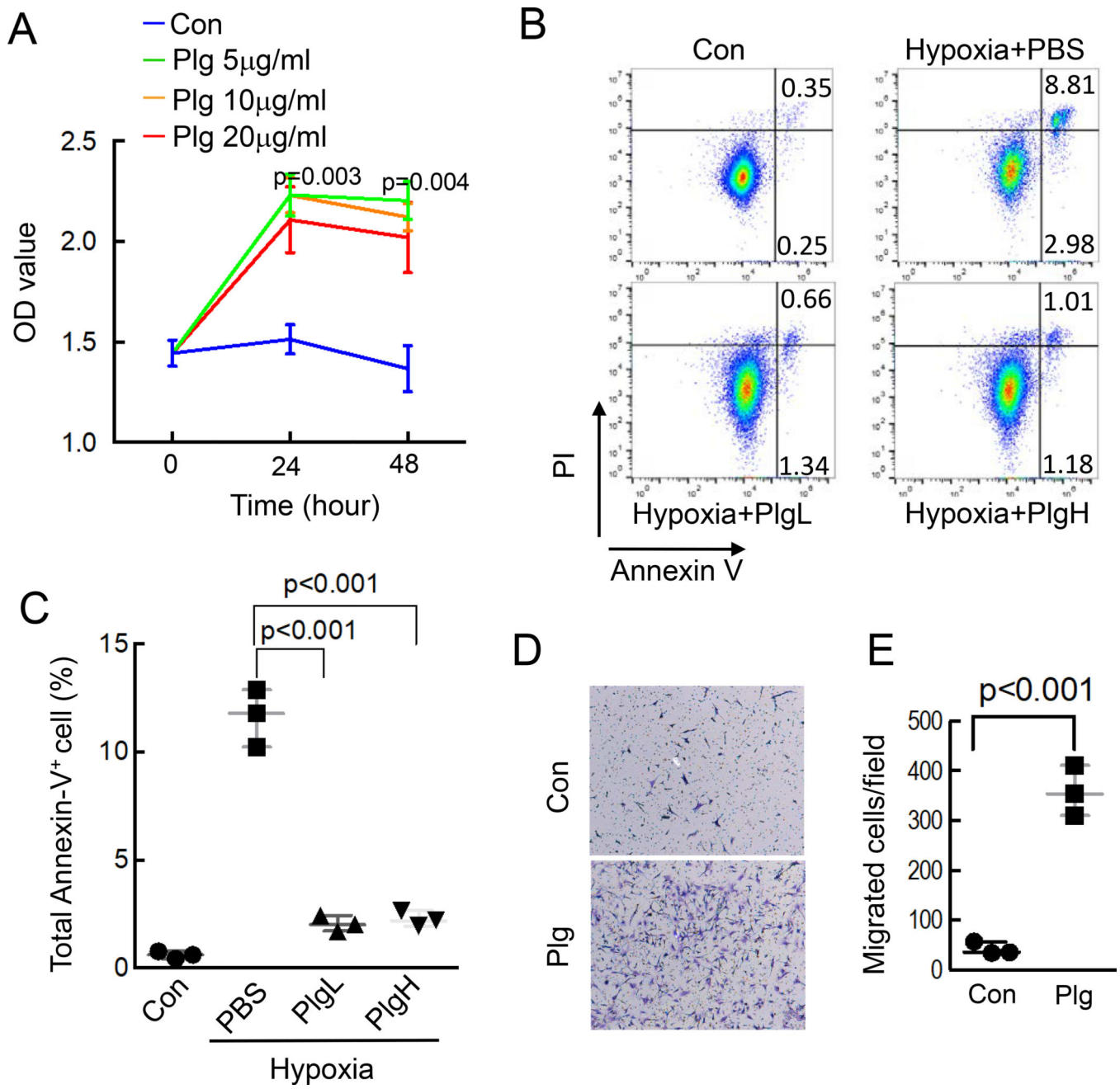

Figure 7. Plg regulates the proliferation, migration, and survival of periosteal progenitors.

(A) Periosteal progenitors were treated with or without Plg under hypoxia (5% O_2) condition. Cell proliferation was determined by MTS. Values are mean ± SEM. p value was analyzed by comparing con group versus Plg(10 μg/ml) group (B) Periosteal progenitors were treated with or without Plg under hypoxia (2% O_2) for 48 hours. Cell apoptosis was evaluated by FACS (PlgL, 10 μg/ml; PlgH, 20 μg/ml) (C) Quantification of percentage of apoptotic cells. (D) Periosteal progenitors were seeded on transwell membranes and migration was induced with 1% FBS as a chemoattractant. Migrated cell in the bottom side

of membrane were stained and representative images were shown. (E) Quantification data of migrated cells. Values are mean ± SEM.

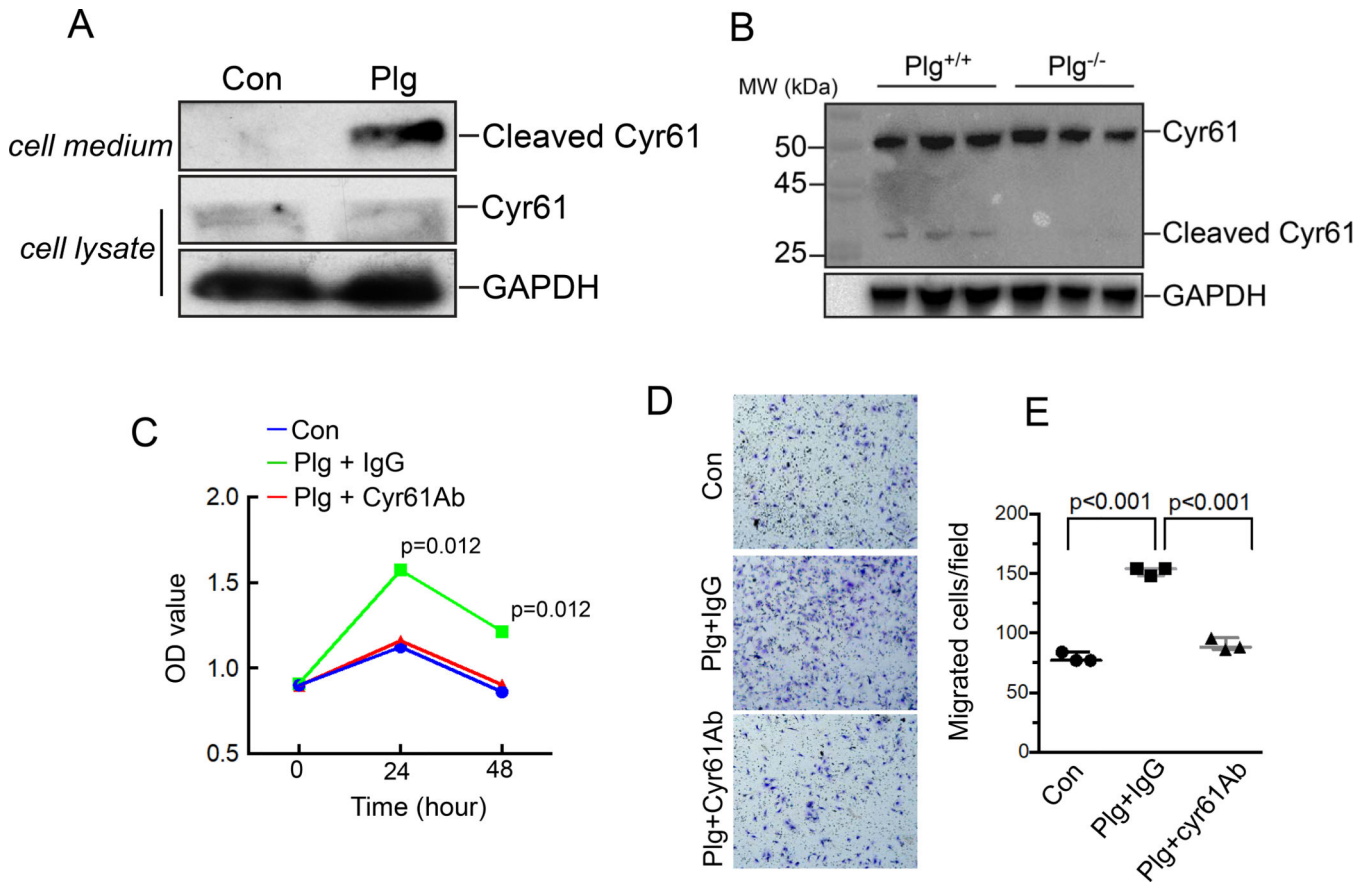

Figure 8. Plasminogen activated Cyr61 by cleavage to promote periosteal progenitor proliferation and migration.

(A) Periosteal progenitors were treated with or without Plg (20 μg/ml) for 24 hours, culture medium and cell lysate were subjected to western blotting assay. (B) Fracture tissues from WT and Plg-KO mice one week after fracture surgery were lysed and subjected to western blotting assay. (C) Periosteal progenitors were treated with PBS or Plg (20 μg/ml) plus IgG or Plg (20 μg/ml) plus anti-Cyr61 antibody under 5% hypoxia. Cell proliferation was determined by MTS assay. Values are mean ± SEM. p value was analyzed by comparing Plg plus IgG group versus Plg plus Cyr61 antibody group. (D) Periosteal progenitors were seeded on transwell membranes and treated with PBS or Plg plus IgG, or Plg plus anti-Cyr61 antibody. 1% FBS was used as chemoattractant in all groups. Migrated cell in the bottom side of membrane were stained and representative images were shown. (E) Quantification data of migrated cells. Values are mean ± SEM.

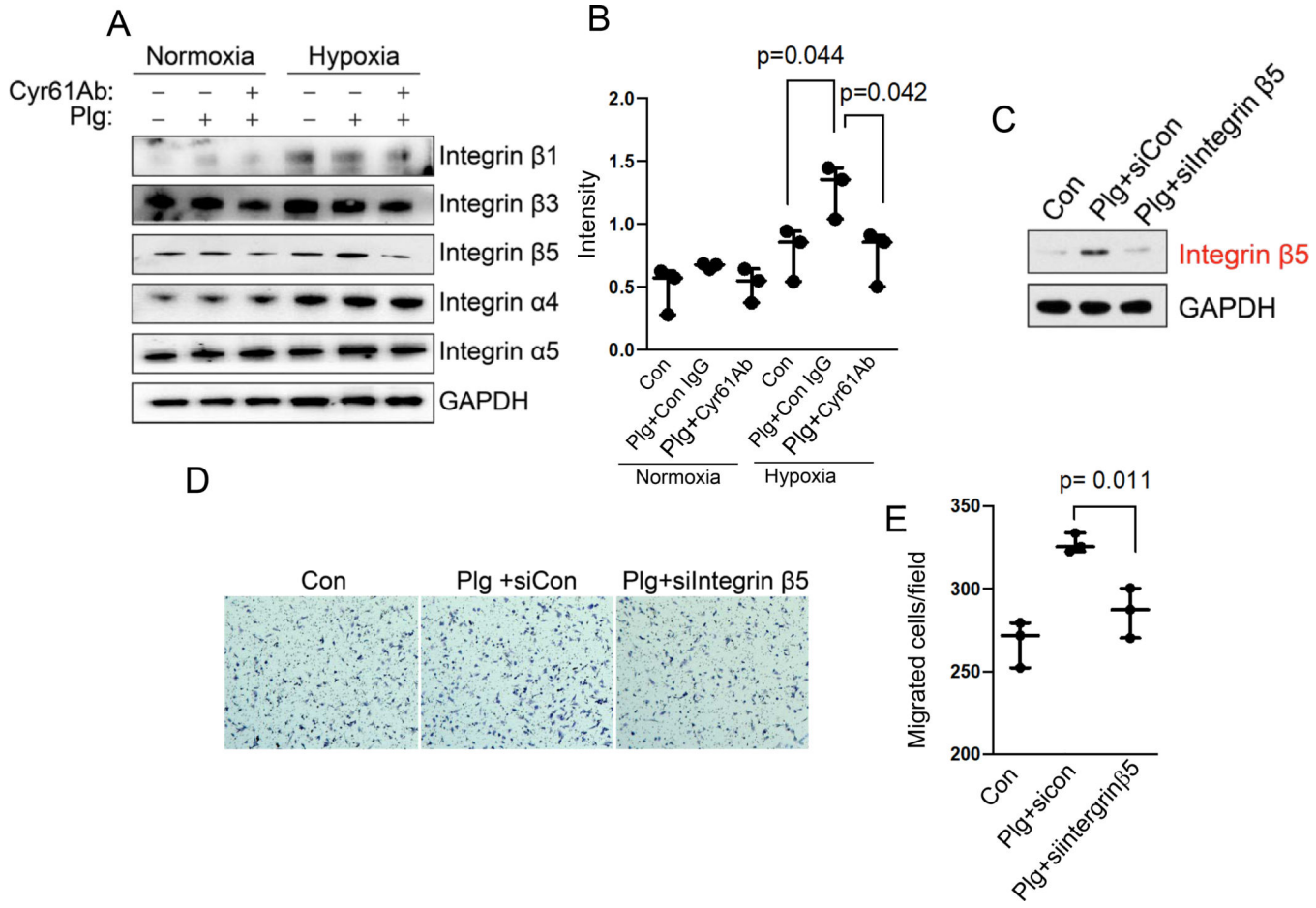

Figure 9. Plg /Cyr61 regulates cell migration through Integrin β5.

(A) Periosteal progenitors were treated with Plg or Plg plus anti-Cry61 antibody under normoxia or hypoxia and cell lysate were subjected to western blotting assay. (B) Quantification data of **Integrin β5** band intensity. Values are mean ± SEM. (C) Periosteal progenitors were treated with con siRNA and Integrin β5 siRNA and cell lystate were subjected to western blotting assay. (D) Periosteal progenitors were seeded on transwell membranes and treated with PBS or Plg plus con siRNA, or Plg plus Integrin β5 siRNA. 1% FBS was used as chemoattractant in all groups. Migrated cell in the bottom side of membrane were stained and representative images were shown. (E) Quantification data of migrated cells. Values are mean ± SEM.

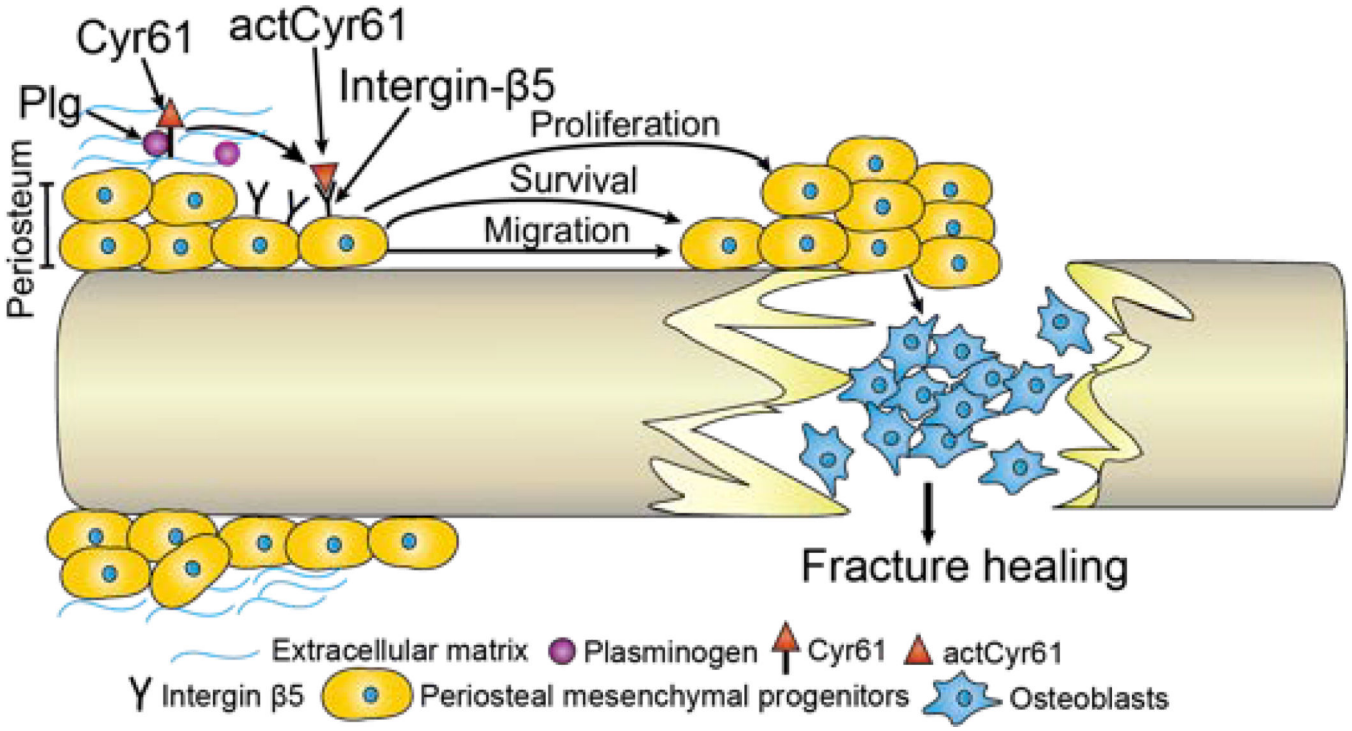

Figure 10. A schematic model.

In fracture microenvironment, Plg cleaves periosteal mesenchymal progenitor-derived Cyr61 into a matrix-free active form, actCyr61. ActCyr61 may bind to Integrin β5 in periosteal mesenchymal progenitors and promotes their migration, survival and proliferation, and therefore enhances bone repair after fracture.